Design and Analysis of an Isolated Bidirectional Dual Active Bridge (DAB) DC-DC Converter with Battery to Grid Capability

Soham Gandhi[1], Ramchandra Kunale[2], Penam Borkar[3], Om Gundawar[5], Prof. Pabitra Guchhait[6]
[1,2,3,4,5,6]*Dept. of Electrical Engineering, G H Raisoni College of Engineering and management, Pune, Maharashtra, India*

***Abstract*— Bidirectional power transfer is essential in emerging electric vehicle charging and distributed battery storage systems, where energy must be exchanged between a high-voltage DC supply and a battery. An isolated Dual Active Bridge (DAB) DC-DC converter is developed and evaluated to enable this bidirectional operation through phase-shift modulation between the primary and secondary full bridges. A concise analytical model is formulated using standard DAB power-phase and inductor-voltage relations to describe the behavior of Grid-to-Battery (G2B) and Battery-to-Grid (B2G) modes. The model is implemented in MATLAB/Simulink using practical parameters, including an 800 V DC input, a 500 V transformer output and a 450 V battery interface at a switching frequency of 100 kHz. The simulation demonstrates stable and controllable power flow in both directions, achieving approximately 10 kW transfer at a phase shift of 22.5° with accurate current polarity and waveform shape. The work provides a clear operational understanding of phase-shift control, bidirectional current behavior, and mode transition in DAB converters, supporting their use in EV-charging infrastructure, battery-energy storage systems, and B2G applications.**

***Index Terms*— Dual Active Bridge (DAB), High-Frequency Transformer, Bidirectional DC-DC Converter, Battery-to-Grid (B2G), Phase-Shift Modulation**

I. INTRODUCTION

The accelerating transition toward electric vehicles (EVs) and distributed energy resources has created new opportunities and challenges in power electronic interfaces that connect batteries, renewable sources, and smart grids. Traditional unidirectional EV chargers, designed primarily for grid-to-vehicle energy transfer, offer limited functionality and are unable to support emerging concepts such as Vehicle-to-Grid (V2G) and Battery-Energy-Storage-Assisted grid services. As the penetration of EVs rises, stationary chargers and onboard power converters must evolve into bidirectional systems with controllable power exchange, galvanic isolation, compact size, and high conversion efficiency.

Bidirectional isolated DC–DC converters play a pivotal role in this paradigm by enabling flexible power transfer between high-voltage DC buses and battery systems without compromising safety. Among the available topologies, the Dual Active Bridge (DAB) converter has emerged as a compelling choice due to its soft-switching capability, zero-voltage switching potential, high power density, and symmetrical port structure. Its ability to reverse power flow merely by altering the phase shift between Hbridge switching signals eliminates the need for mechanical switching or additional hardware layers, which simplifies control and enhances reliability. These attributes make the DAB converter well-suited for V2G, G2V, and renewable-integrated charging architectures where bidirectional, isolated, and dynamically controllable power conversion is essential. However, despite its promising characteristics, the practical implementation of DAB converters still faces challenges related to optimal phase-shift control, current stress, transformer parasitics, and efficiency under varying operating conditions. As EVs are increasingly expected to support grid stability services—such as peak shaving, load balancing, and renewable-energy buffering—there is a pressing need to refine the performance of bidirectional converters and bridge the gap between theoretical modelling and real-world deployment. Motivated by these developments, this work presents the modelling, simulation, and analysis of an isolated bidirectional DAB DC–DC converter that supports Battery-to-Grid (B2G) interaction while retaining Grid-to-Battery (G2B) charging capability under a single universal topology.

II. LITERATURE REVIEW

Recent research emphasizes the importance of DAB converters as a core technology enabling EV-to-grid interoperability and high-efficiency bidirectional charging. Rajender et al. [1] demonstrated that isolated DAB converters can achieve regulated bidirectional power flow using phase-shift modulation, although their work primarily focuses on modelling and lacks extensive analysis of grid-supporting behaviour. Singh et al. [2] explored a Level-3 EV charging system using a bidirectional DAB converter and reported high efficiency under extended phase-shift operation; however, the study provides limited insight into transformer parasitic effects that influence current ripple and switching stress.

Enhancements in converter efficiency using wide-bandgap switches have been investigated in [3], where an SiC-based DAB system was shown to improve charging performance and reduce switching losses. Although the approach is technologically advanced, it increases system cost and complexity, which may limit adoption in lowto-mid-power EV charging applications. Similarly, Naseem and Seok [4] reviewed bidirectional power electronic converters for regenerative EV systems, identifying control responsiveness as a major limitation during dynamic power reversals. [3] M. T. Shahed, M. M. Haque, and S. Akter (2023) designed an IoT-enabled solar energy management system to improve smart grid reliability and power quality. The study focused on real-time solar monitoring and cloud-based visualization for efficient renewable energy utilization.

Advanced modulation schemes are explored in [5], where hybrid single-phase-shift techniques expand the zero-voltage switching range. While such strategies enhance efficiency, their implementation demands precise timing and increased computational burden. Another significant direction is renewable-integrated bidirectional charging, where Kumar et al. [6] examined DAB-based converters interfaced with solar-assisted EV charging infrastructure. Although promising, their topology does not explicitly consider B2G dispatch control, which restricts its applicability for smart-grid participation.

Recent studies also highlight the importance of improving current shaping and control coordination in DAB converters. Liu et al. [7] introduced adaptive modulation for dynamic grid scenarios, yet the work lacks detailed transformer modelling, reducing its suitability for isolated architectures. Finally, Patel and Sharma [8] discuss practical challenges in deploying DAB converters for smart grids, identifying the absence of unified design guidelines for bidirectional control, leakage inductance selection, and transformer sizing.

III. SYSTEM ARCHITECTURE AND MODELLING

The system considered in this work is an isolated Dual Active Bridge (DAB) DC-DC converter designed to achieve controlled bidirectional energy exchange between a high-voltage DC source and a lower-voltage battery system. The converter adopts two actively switched full bridges connected through a high-frequency transformer that provides provides galvanic isolation and voltage adaptation. Bidirectional power flow is enabled by introducing a commanded phase shift between the primary and secondary switching functions, allowing the same hardware to support both charging and discharging modes.

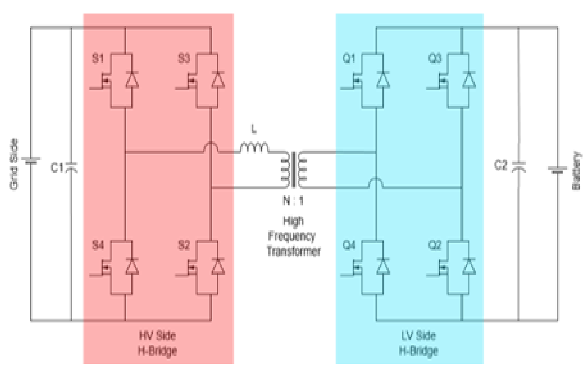

Fig. 1. System architecture of the isolated DAB DC-DC converter.

3.1 System Architecture

The converter architecture consists of the following functional units:

High-Voltage Full Bridge (Primary Side)

The primary bridge is supplied by an 800 V DC source and produces a high-frequency square-wave voltage that excites the transformer. Its switching pattern leads or lags the secondary bridge depending on the intended power direction.

High-Frequency Isolation Transformer

A transformer rated at 800 V / 500 V provides galvanic isolation between the grid-side and battery-side ports. The turns ratio of the transformer, denoted as N, is obtained from the ratio of the primary-side DC level to the rated secondary voltage. This transformer ensures safe isolation and enables efficient high-frequency operation.

Total Series Inductance

Energy transfer between the two bridges is governed by the current flowing through a series inductance placed in the transformer path. In the implemented system, the total inductance is

$$L = L_{p,lk} + L_{ext}$$

where $L_{p,lk} = 1.7 \times 10^{-5}$ His the transformer primary leakage inductance and $L_{ext} = 1.5 \times 10^{-5}$ His the external series inductor. The total inductance, therefore, is

$$L = 3.2 \times 10^{-5}\ \text{H}.$$

This inductance shapes the high-frequency current and plays a central role in regulating the transferred power.

Low-Voltage Full Bridge (Secondary Side)

The secondary bridge interfaces with the battery through a DC link nominally around 450 V. By advancing or delaying its switching signals relative to the primary bridge, the direction of power flow-G2B or B2G-is controlled.

DC-Link Capacitors

Both DC ports include capacitors to support voltage stability and reduce high-frequency ripple. These capacitors act as local energy buffers and maintain smooth DC voltages during switching transitions.

3.2 Modelling Approach

The DAB is modelled using the conventional first-harmonic approximation (FHA), where the square-wave bridge voltages are represented by their fundamental components. The series inductance behaves as the main energy-transfer element, and its current evolves in a piecewise-linear manner within each switching period.

Bidirectional operation is established by controlling the phase shift ϕ(positive or negative) between the primary and secondary bridge voltages. A positive phase shift results in power transfer from the high-voltage side to the battery (G2B), while a negative phase shift reverses the power direction (B2G).

Power-Phase Relationship

The average transferred power under FHA is:

$$P(\phi) = \frac{V_{HV}\ N\, V_{batt}}{2\pi^2 f_s L}\ \phi(\pi - \phi), \qquad N = \frac{V_{HV}}{V_{sec}} \quad (1)$$

The corresponding phase shift for a specified power level follows:

$$\phi^2 - \pi\phi + \frac{P}{K} = 0, \qquad K = \frac{V_{HV}\ N\, V_{batt}}{2\pi^2 f_s L} \quad (2)$$

These equations describe how the power flow varies with voltage levels, total inductance and transformer turns ratio.

Port Currents

The average DC currents at the converter interfaces are []:

$$I_{HV} = \frac{P}{V_{HV}}, \qquad I_{batt} = \frac{P}{V_{batt}} \quad (3)$$

These expressions are used to evaluate conduction stress on the switching devices and the inductor.

Differential Inductor Voltage

The inductor experiences the fundamental voltage difference between the primary and the reflected secondary voltage:

$$V_{diff} = V_{HV} - NV_{batt} \quad (4)$$

This voltage determines the slope of the inductor current during the conduction interval of each switching cycle.

Inductor Ripple Modelling

The peak-to-peak inductor current ripple is expressed as:

$$\Delta \mathrm{I_{pp}} = \frac{V_{diff}\phi}{2\pi f_s L} \quad (5)$$

Its RMS value is:

$$\mathrm{I_{ripple,rms}} = \frac{\Delta \mathrm{I_{pp}}}{2\sqrt{3}} \quad (6)$$

and the inductor RMS current is:

$$\mathrm{I}_{L,rms} = \sqrt{I_{HV}^2 + I_{ripple,rms}^2} \quad (7)$$

These relations are essential for estimating copper losses and verifying current stress.

Conduction Loss Expression

The conduction loss associated with the inductor resistance is:

$$\mathrm{P_{L,loss}} = \mathrm{I_{L,rms}^2 R_L} \quad (8)$$

This expression plays a role in thermal assessment and overall efficiency analysis.

Inductance Requirement for Ripple Control

If a target ripple magnitude is defined, the required inductance is:

$$\mathrm{L} = \frac{\mathrm{V_{diff}}\phi}{2\pi \mathrm{f_s} \Delta \mathrm{I_{pp,target}}} \quad (9)$$

This equation is used to justify the chosen inductance in ripple-critical designs.

PWM Delay Implementation for Phase Shift

Digital control of phase shift is achieved through a programmable delay:

$$t_{delay} = \frac{\phi_{deg}}{360} T, \qquad T = \frac{1}{f_s} \quad (10)$$

A negative delay corresponds to battery-to-grid operation.

IV. OPERATING MODES OF THE BIDIRECTIONAL DAB CONVERTER

The Dual Active Bridge converter supports two principal operating modes depending on the sign and magnitude of the commanded phase shift between the primary and secondary full bridges. As established in Section 3, the average transferred power, inductor voltage, current ripple and PWM delay are governed by Eqs. (1)-(10). In this section, the same analytical expressions are interpreted for the two power-flow directions: Grid-to-Battery (G2B) and Battery-to-Grid (B2G). Only the physical behaviour, waveform characteristics and direction of energy transfer differ between the two modes, while the underlying equations remain unchanged.

4.1 Grid-to-Battery (G2B) Operation

In G2B operation, the converter transfers energy from the high-voltage DC port to the battery-side DC link. This occurs when the primary full bridge leads the secondary, resulting in a positive phase shift $\phi > 0$.

According to the power-phase relationship defined in Eq. (1), a positive phase shift produces a positive power transfer from the HV port toward the battery. The exact value of ϕrequired to achieve a desired power level follows the quadratic relation of Eq. (2).

The average port currents during charging correspond to Eq. (3), where the HV-side current represents the input and the battery-side current represents the delivered charging current.

During G2B charging, the differential inductor voltage defined in Eq. (4) becomes positive because the primary bridge voltage leads the reflected secondary bridge voltage. This positive V_{diff}produces an increasing inductor current slope during the conduction interval. The corresponding ripple and RMS current characteristics follow Eqs. (5)-(7).

The positive phase shift is implemented through a positive PWM delay, as defined in Eq. (10). The resulting waveforms typically show the primary voltage leading the secondary voltage, followed by a rising triangular inductor current with a stable average component.

4.2 Battery-to-Grid (B2G) Operation

In B2G mode, the converter delivers power from the battery back to the high-voltage DC port. This mode becomes active when the secondary bridge leads the primary, resulting in a negative phase shift $\phi < 0$.

The same power-phase equation (Eq. (1)) governs the magnitude of power transfer, but the sign of the phase shift reverses, causing power to flow from the battery toward the HV port. The corresponding solution for ϕcontinues to follow Eq. (2), with the negative value indicating reverse operation.

The average port currents reverse their direction according to Eq. (3), where the battery current represents discharge and the HV-side current represents delivered grid or DC-bus power.

The differential inductor voltage from Eq. (4) becomes negative in this mode because the reflected secondary voltage leads the primary. This results in a negative slope in the inductor current waveform. The ripple and RMS current characteristics remain governed by Eqs. (5)-(7) since ripple magnitude depends on the absolute slope and conduction interval, not the direction of

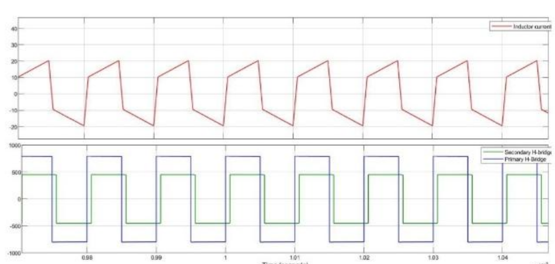

current flow.

The B2G mode is implemented by applying a negative PWM delay, which directly follows the relation in Eq. (10).

V. RESULTS AND DISCUSSION

The operational behaviour of the proposed Dual Active Bridge converter was analyzed under both Grid-to-Battery (G2B) and Battery-to-Grid (B2G) modes using the Simulink model developed in Section 5. The objective of this section is to present the steady-state waveforms, validate the theoretical operation derived in Section 3 and demonstrate the bidirectional power-transfer capability governed by the phase-shift control strategy. The simulated results confirm that the direction and magnitude of power flow are controlled solely through the phase displacement between the two bridges, without requiring any changes in hardware configuration.

Parameter	Symbol	Value	Unit
High-voltage DC source	V_{HV}	800	V
Rated transformer secondary voltage	V_{sec}	500	V
Battery DC voltage	V_{batt}	450	V
Transformer turns ratio	N	1.6	-
Switching frequency	f_s	100,000	Hz
Transformer primary leakage inductance	$L_{p,lk}$	1.7×10^{-5}	H
External series inductance	L_{ext}	1.5×10^{-5}	H
Total series inductance	1.7×10^{-5}	3.2×10^{-5}	H
Primary winding resistance	R_p	0,043	Ω
External inductor series resistance	R_L	0.016	Ω
Secondary winding resistance	R_s	1×10^{-6}	Ω
Magnetizing inductance	L_m	$720\times10^{-}$	H
Magnetizing core resistance	R_m	10×10^{3}	Ω
HV-side capacitor	C_{HV}	$100\times10^{-}$	F
LV-side capacitor	C_{LV}	2000×1(	F
Capacitor ESR (both ports)	R_C	0.001	Ω
Phase shift (simulation value)	ϕ	22.5	°

5.1 Grid-to-Battery (G2B) Operation

In G2B mode, the primary bridge leads the

Fig. 2: Inductor Current & Bridge Voltages Waveform - G2B Mode

secondary through a positive phase shift. As a result, the differential voltage across the series inductance becomes positive, producing a rising inductor current waveform. This behaviour is consistent with the theoretical expression for differential voltage provided in Eq. (4), and with the power-phase relationship in Eq. (1), which predicts positive power flow toward the battery when $\phi > 0$.

The waveform in Fig. 5 shows a triangular inductor current profile, confirming that the inductance is functioning as the main energy-transfer element, as modelled earlier. The current rises during the conduction interval of the primary bridge and delivers energy to the battery. The output power settles to a stable positive value, indicating successful charging operation.

Fig. 3: Output Power Waveform - G2B Mode

From Fig. 3, it can be observed that the power flow reaches a steady level without oscillations, demonstrating effective control of the converter dynamics. The voltage across the battery remains regulated, while the current establishes the charging direction predicted by Eq. (3).

5.2 Battery-to-Grid (B2G) Operation

When the phase shift becomes negative, the secondary bridge leads the primary, reversing the polarity of the differential voltage. This produces a negative slope in the inductor current, resulting in energy flowing from the battery toward the high-voltage DC bus. This observation agrees with the theoretical behaviour defined in Eq. (4), where the sign change in V_{diff} directly changes the power transfer direction in Eq. (1).

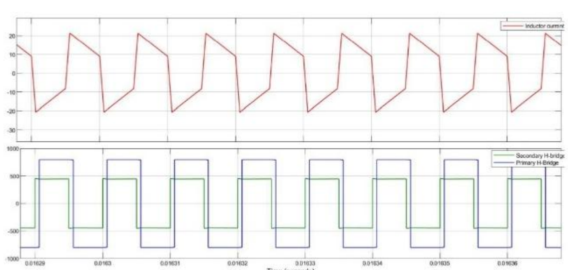

Fig. 4: Inductor Current and Bridge Voltages in B2G Mode

The inductor current waveform now exhibits a downward slope, confirming the reversal of energy transfer. No structural or component-level modifications are required to switch the operating mode, reinforcing the dual-active nature of the topology.

Fig. 5: Input/Output Voltage and Current Waveforms in B2G Mode

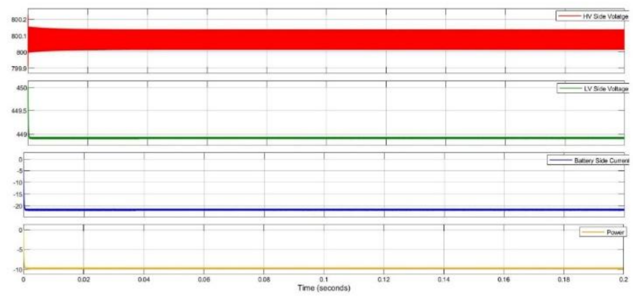

Fig. 5 verifies that the battery current reverses direction while the high-voltage bus receives power, demonstrating the grid-support functionality of the

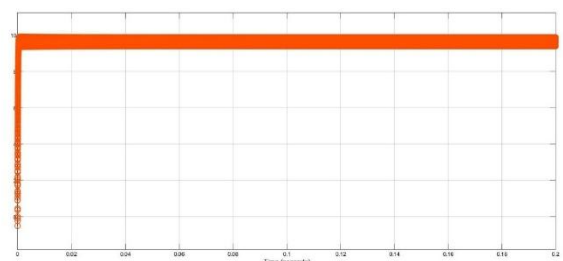

proposed system. The waveforms maintain a smooth transition and achieve stable steady-state values, indicating that the phase shift alone is sufficient for directional control.

5.3 PWM Phase-Shift Verification

The PWM signals of both bridges were observed to confirm the implementation of the phase-shift mechanism directly through the Pulse Generator blocks. The waveforms validate the theoretical delay relationship defined in Eq. (10). In G2B mode, the HV bridge pulses lead those of the LV bridge, whereas in B2G mode, the order reverses.

This observation confirms that software-based phase manipulation is a reliable control technique and eliminates the need for complex switching or modulation hardware.

5.4 Discussion

The simulated waveforms demonstrate that:

- The direction of power flow can be regulated entirely by the sign of the phase shift
- The magnitude of transferred power follows the theoretical dependence on phase shift, inductance and DC port voltages
- Inductor current behaviour (slope and polarity) directly reflects the analytical expressions in Eqs. (4)-(7)
- Both G2B and B2G operations share identical hardware, validating the dual-active nature of the topology
- The converter achieves stable steady state in both directions, showing excellent controllability and predictable dynamic response

These results confirm that the theoretical model and simulation are in agreement, validating the mathematical expressions developed earlier and proving the suitability of the proposed DAB converter for electric-vehicle charging and grid-support functions.

VI. CONCLUSION & FUTURE SCOPE

The isolated bidirectional Dual Active Bridge DC–DC converter analysed in this work demonstrates reliable Grid-to-Battery (G2B) and Battery-to-Grid (B2G) operation using phase-shift modulation without any hardware reconfiguration. The simulation results confirmed the theoretical power–phase relationship, validated the inductor current behaviour, and verified stable bidirectional power flow, indicating that the total series inductance and transformer turns ratio significantly influence the converter's dynamic response. These characteristics reinforce the suitability of the DAB topology for electric vehicle charging, distributed storage systems, and emerging smart grid environments requiring secure and flexible power exchange. Although the system performs effectively, the present open-loop control limits its adaptation to varying load and grid conditions. Future enhancements include implementing closed-loop control for improved regulation, enabling grid-interactive functions such as peak load management and frequency support, and developing a hardware prototype to experimentally validate performance. Incorporating advanced switching devices and integrating renewable sources may further expand the converter's applicability to next-generation EV charging and decentralized energy infrastructures.

REFERENCES

[1] Rajender, J., Dubey, M., Kumar, Y.: Design and analysis of a high-efficiency bi-directional DAB converter for EV applications. Scientific Reports, 14(1), 2024.

[2] Singh, N., Tomar, A., Sehgal, D.: High-efficiency bidirectional Dual Active Bridge DC/DC converter for Level-3 electric vehicle charging. Advances in Research, 26(1), 274–282, 2025.

[3] Kumar, K.N., Miśkiewicz, R., Trochimiuk, P., Rąbkowski, J., Peftitsis, D.: Comparative analysis of SiC-based isolated bidirectional DC/DC converters for modularized off-board EV charging systems with bipolar DC link. Electronics, 14(22), 4522, 2025.

[4] Naseem, H., Seok, J.K.: Recent advances in bidirectional converters and regenerative braking systems in electric vehicles. Actuators, 14(7), 347, 2025.

[5] Esteve, J.M., Marcano, J., Gago, M.: Improved phase-shift modulation strategies in Dual Active Bridge converters for EV charging. IEEE Trans. Transportation Electrification, 10(2), 2024.

[6] Kumar, R., Sen, A., Bhowmick, P.: Renewable-integrated DAB converter for distributed EV charging systems. Energy Conversion and Management, 310, 2024.

[7] Liu, X., Zhang, D., Huang, Y.: Adaptive phase-shift controlled DAB converters for gridinteractive EV systems. IEEE J. Emerging and Selected Topics in Power Electronics, 12(1), 2025.

[8] Patel, R., Sharma, V.: Control challenges and implementation issues of bidirectional DAB converters in smart grids. International Journal of Smart Energy Systems, 18(4), 2024.

[9] Chandra, K., Rao, G., Banerjee, S.: Development and efficiency analysis of Dual Active Bridge with single-phase shift modulation control. IET Power Electronics Research, 13(5), 901-912, 2025.

[10] Wu, Q., Wang, Z., Li, G., Chen, Y.: A fully isolated triple-port bidirectional DC-DC converter based on integration of Dual Active Bridge and LLC resonant converter. In: Proc. IEEE International Symposium on Industrial Electronics, pp. 1-6, 2025.

[11] Wu, Q., Wang, Z., Li, G., Chen, Y.: A fully isolated triple-port bidirectional DC-DC converter based on integration of Dual Active Bridge and

LLC resonant converter. In: Proc. IEEE International Symposium on Industrial Electronics, pp. 1-6, 2025.
[12] Liu, X., Zhang, D., Huang, Y.: Adaptive phase-shift controlled DAB converters for gridinteractive EV systems. IEEE Journal of Emerging and Selected Topics in Power Electronics, 12(1), 2025.
[13] Khan, A., Rehman, F., Alam, M.: All-SiC based bidirectional isolated DC-DC converter for next-generation V2G chargers. IEEE Transactions on Power Electronics, 39(3), 2024.
[14] Zhang, L., Hu, S., Li, Q.: Dual-bridge isolated converter with reduced current stress for BESS-assisted EV charging. Journal of Energy Storage Systems, 45, 2025.
[15] Patel, R., Sharma, V.: Control and implementation challenges of DAB converters in smart grids. International Journal of Smart Energy Systems, 18(4), 2024.